2023

Fully 3D-Printed Hemispherical Dielectric Resonator Antenna for C-band Applications

Jakub Przepiorowski
Technological University Dublin, Ireland, jakub.przepiorowski@tudublin.ie

Irina Munina
Trinity College Dublin, ireland

Max Ammann
Technological University Dublin, max.ammann@tudublin.ie

See next page for additional authors

Funder: 10.13039/501100001602-Science Foundation Ireland

Authors

Jakub Przepiorowski, Irina Munina, Max Ammann, and Daniel Trimble

Fully 3D-Printed Hemispherical Dielectric Resonator Antenna for C-band Applications

Jakub Przepiorowski[1], Irina Munina[2], Max J. Ammann[1], Daniel Trimble[2]
[1] Antenna and High Frequency Research Centre, TU Dublin, Ireland, jakub.przepiorowski@ieee.org
[2] Dept. of Mechanical, Manufacturing & Biomedical Engineering, Trinity College Dublin, Ireland, muninai@tcd.ie

***Abstract*— This paper investigates the 3D printing of a hemispherical dielectric resonator antenna (DRA) on a ground plane made from a 3D printed conductive material. The DRA is designed to operate in the C-band (3700 – 4200 MHz) and is intended for satellite communication (SATCOM) applications. The proposed antenna prototype achieved a -10 dB bandwidth of 12.2% with an average and peak gain of 4.69 dBi and peak gain of 5.39 dBi respectively.**

***Index Terms*—dieletric resonator antenna, hemispherical, high efficiency, 3D, SATCOM**

I. Introduction

The shapes and materials of dielectric resonator antennas (DRA) can be very diverse offering a high degree of parameter flexibility compared to two-dimensional planar antennas. As DRAs do not use conductive materials to radiate, they are highly efficient antennas especially when using low-loss dielectric materials [1].

The recent advances in 3D-printing technology offers the possibility of manufacturing prototypes using various materials at a reduced cost, increased throughput rate and reduced manufacturing process complexity [2]. One of the advantages of 3D-printing compared to a standard machining process, is that complex and irregular shapes can be fabricated in a much easier and faster way. This feature can be useful when designing non planar antennas such as DRAs which are three-dimensional objects. [3].

Many 3D-printed antennas exist in the literature [4] [5], however most "fully" 3D-printed DRA examples describe the process of only fabricating the dielectric resonator and using it with a prefabricated substrate such as standard FR-4. However, with the emergence of new filament materials [6] the ground plane of the DRA can also be 3D-printed meaning that the only additional component of the antenna will be the RF connector.

The high efficiency property of DRAs makes them a good candidate for low power, fixed and mobile satellite communication (SATCOM) terminals where a high efficiency system is required for the terminal to operate over long periods when self-powered in off-grid and remote locations. With the widespread roll-out of 5G, there is an emergence of new terrestrial and SATCOM services with various applications in frequency bands such as the newly reformed C-band (3700 – 4200 MHz) [7].

In this paper a fully 3D printed linearly-polarized DRA is presented. The antenna operates in the C-band (3700 – 4200 MHz). The prototype antenna was fabricated using two different materials, a ceramic dielectric material and a conductive filament. Different design parameters are explained in Section II and the measured and simulated results are compared in Section V. Section III describes how the presented linear antenna can be converted into a circularly-polarized antenna for use in SATCOM applications. The fabrication process is explained in Section IV.

II. Antenna design

A. Antenna design

As shown in Figure 1, the DRA consists of two main components, the dielectric resonator, and a reflective metallic ground plane. The dielectric resonator in this case is a hemisphere with a radius of 12.25 mm. The metallic ground plane is a 40x40 mm square with a smaller hemisphere of radius 4.8 mm placed in the centre. The structure is excited using a single SMA connector with the probe length of 7.3 mm. The length of the connector probe was optimized for performance as it influenced the matching.

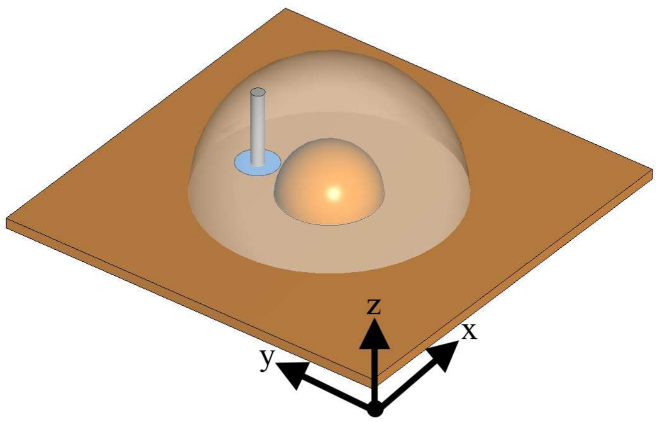

Fig 1. Simulated 3D model.

The position of the probe feed determines the radiation pattern of the antenna. In this design, the connector probe was placed 7.8 mm from the centre.

B. The effect of the inner metallic hemisphere

As described above, a metallic hemisphere was included in the centre of the metallic ground plane. This inner sphere provides important benefits. Firstly, it increases the impedance bandwidth of the antenna as shown in Figure 2 where two models, with and without the inner hemisphere, are compared. The model with the inner hemisphere provides a S11 -10 dB bandwidth of 435 MHz while the model without the hemisphere had a bandwidth of 268MHz.

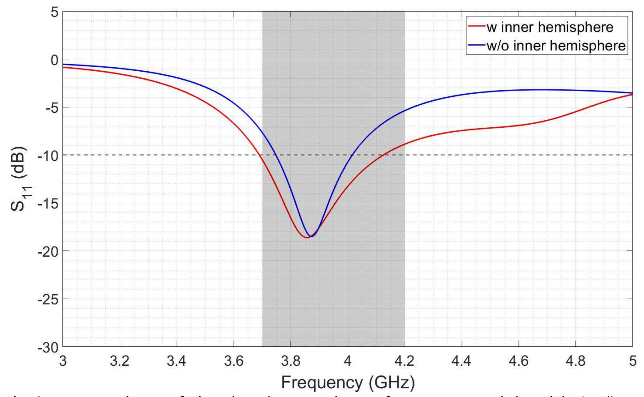

Fig 2. Comparison of simulated return loss of antenna models with (red) and without (blue) inner metallic hemisphere.

Other impedance bandwidth broadening techniques exist in the literature, those include using multiple dielectric materials with different dielectric constants, adding airgaps, or using different feeding techniques.

Another advantage that the metallic hemisphere provides, is a better gain distribution over the desired frequency range as shown in Figure 3. Both models give the same average gain over the desired band, but the metallic hemisphere model has a gain variation of 0.45 dB whereas the model without the metallic hemisphere has a variation of 1.35 dB.

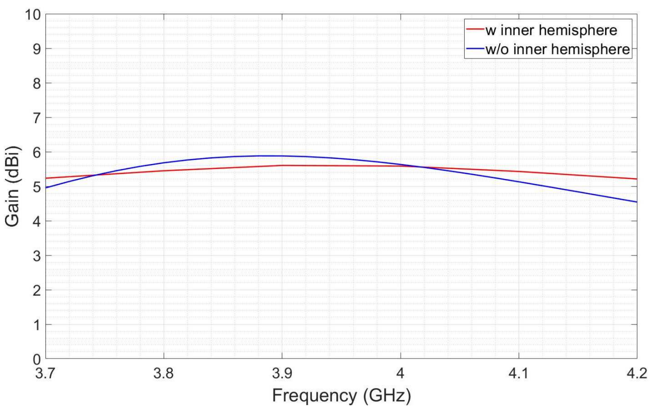

Fig 4. Gain plot over desired frequency band.

III. CIRCULAR POLARIZATION

Due to the parameter flexibility offered by DRAs, circular polarization can be generated in numerous ways. The shape of the DRA can determine the polarization, the feeding technique, the feed position or even the addition of extra parasitic elements around the dielectric resonator [8]. The addition of parasitic elements can be realized relatively easily with the use of 3D-printing.

The addition of a second port with an angular separation of 90° degrees from the first port, is a common way of generating circular polarization in symmetrical shapes. Although dual excited antennas can give wide axial-ratio bandwidth, they require extra hardware to create the 90° degree phase shift between the ports. Figure 4 shows a dual feed design of the proposed model.

Plotted below are the simulated axial-ratio and S_{11} plots. The S_{11} plot shows a -10 dB bandwidth of 24.28% (4737 – 3711 MHz). The axial-ratio can be seen to be < 3dB over the desired band (3700 – 4200 MHz).

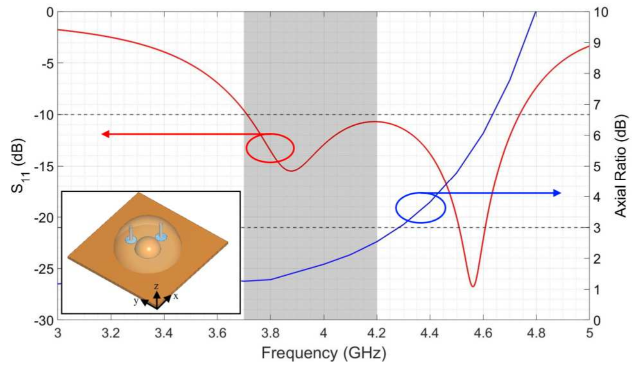

Fig 3. S_{11} and axial ratio plots of the simulated circularly polarized model.

IV. 3D FABRICATION PROCESS

The main objective of this paper was to present a fully 3D printed DRA antenna, meaning that all antenna components except the SMA connector are 3D printed. As mentioned in Section II, the antenna consists of two components, a metallic ground reflector, and a dielectric hemisphere. A fused filament fabrication (FFF) process was used to fabricate the prototype. FFF is an additive manufacturing (AM) process in which materials are extruded through a heated nozzle, deposited layer-by-layer and merged together to create a three-dimensional object. It is one of the most used AM processes due to its low cost and complexity. Both antenna components were printed using the Original Prusa i3 MK3S+ 3D printer. The metallic ground plane was printed using a conductive material Electrifi (ρ = 0.006 Ω cm) [9] and the dielectric hemisphere was printed using PREPERM ABS1200 (ε_r = 12, tanδ = 0.004) [10]. The given resistivity, permittivity and loss tangent values are for solid materials as taken from the datasheets. The two components were friction fitted together during the measurements, but in the future work, a conductive adhesive will be used.

As the temperature of the nozzle increases during the printing process, the resistivity of the Electrifi material increases which in turn causes the conductivity to decrease. Since the conductive material is only used for the ground plane which acts as a reflector, the conductivity of the material is not a critical parameter.

Figure 5 shows the fabricated antenna prototype. The anomalies caused by the 3D printing process such as the thermal expansion of the material and any extra left-over material from the printer nozzle, were fixed by hand using various tools. A smooth and minimal gap was ensured between the dielectric material and the metallic ground plane. The SMA connector was pressure fitted into position and a proper contact between the connector and the ground plane was established.

Due to the issues mentioned above, an airgap was observed between the dielectric hemisphere and the metallic ground plane. This small airgap contributes to a shift in resonance of the DRA to a higher frequency. Another major contributor to the resonance shift is the 3D printing process of high dielectric permittivity materials as it can alter the electromagnetic properties of the materials. Parameters such as printing speed, nozzle temperature, layer height and material infill percentage are all major factors [11]. The main printer parameters used for this prototype are listed in the Table I.

TABLE I. 3D PRINTER SETTINGS

	PREPERM ABS1200	Electrifi
Nozzle Temperature	250 C	182 C
Bed Temperature	110 C	23 C
Printer Speed	10 mm/s	10 mm/s
Infill Percentage	100 %	100 %

Fig 5. Fabricated prototype.

V. EXPERIMENTAL RESULTS AND ANALYSIS

The return loss measurements were performed using a Rhode & Schwarz ZVA40 vector network analyser. The farfield properties of the prototyped antenna were measured in an anechoic chamber. Following is a comparison between the simulated and measured results.

A. Impedance Plot

Figure 6 shows the S11 plots of the simulated and measured results. The simulated and measured -10 dB bandwidth is 11.2% (3688 – 4126 MHz) and 12.2% (3860 – 4360 MHz) respectively.

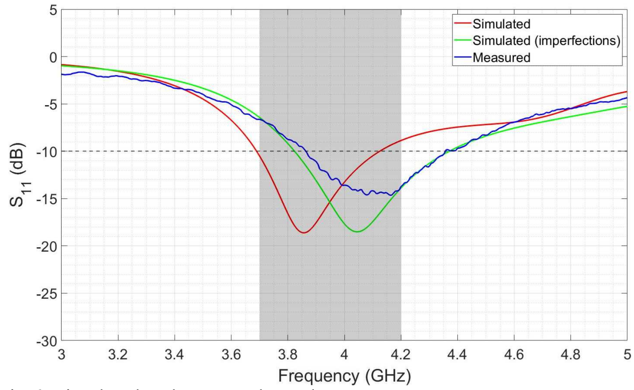

Fig 6. Simulated and measured S_{11} plots.

As mentioned in previous section, the resonance shift is due to minor imperfections in the fabrication process. This also caused the bandwidth to larger than the simulated one. A 3D EM model was made with extra parameters to compensate for the imperfections and match the measured results. An airgap of 0.13 mm was added between the dielectric hemisphere and the ground plane.

B. Radiation Pattern

Figure 7 shows the simulated and measured radiation properties for the x-z plane of the proposed antenna. The simulated results show a beamwidth of 102.7° degrees for the desired model and 105.2° degrees for the model with fabrication imperfections. The measured bandwidth was found to be 100° degrees. All presented patterns were measured at 4 GHz.

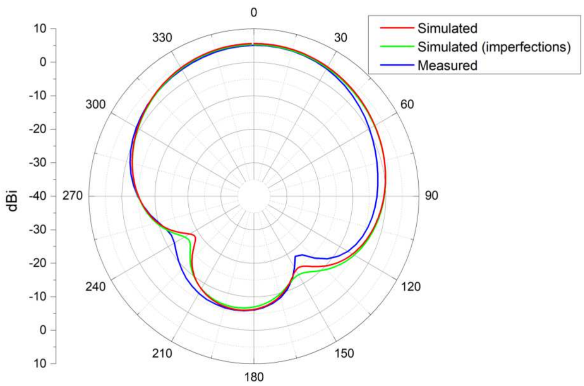

Fig 7. Simulated and measured radiation pattern plots at 4 GHz.

C. *Gain over frequency*

Figure 8 compares the two simulated gain plots, red representing the desired model and green representing a simulated model with fabricating flaws, to the measured plot of the prototype antenna. Over the specified frequency range (3700 – 4200 MHz), the average simulated gain for the desired model was found to be 5.45 dBi, for the model with imperfections to be 4.90 dBi and the measured to be 4.69 dBi. The frequency shift and decrease in peak gain in the green plot closely reflect results in the measured gain plot. The peak gains over the frequency band were found to be 5.62 dBi, 5.40 dBi and 5.39 dBi, respectively.

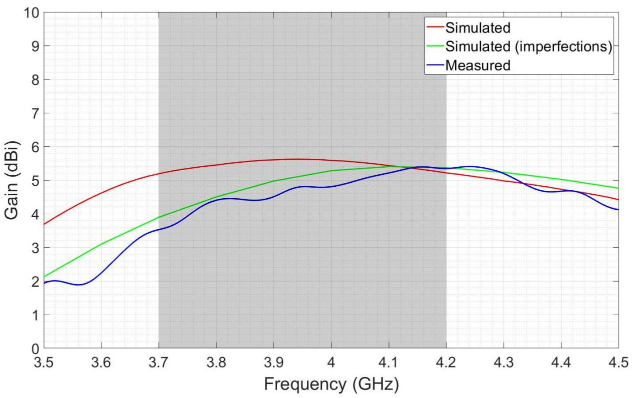

Fig 8. Simulated and measured plots of the gain over the desired frequency band.

VI. Conclusion

A process of 3D-printing a DRA hemispherical antenna along with the metallic ground plane was presented. The entire antenna with the exception of the SMA connector was 3D printed. The proposed antenna operates in the C-band (3700 – 4200 MHz) and has 5G and SATCOM applications. The proposed design obtained an average gain of 4.69 dBi over the frequency range with a peak of 5.39 dBi. The -10 dB impedance bandwidth was measured at 12.2% (3860 – 4360 MHz).

Acknowledgment

This publication has emanated from research supported in part by Science Foundation Ireland under Grant number 18/CRT/6222

Irina Munina was supported by the European Union's Horizon 2020 research and innovation programme under the Marie Skłodowska-Curie grant agreement No. 847402.

References

[1] K.-M. Luk and K.-W. Leung, Dielectric Resonator Antennas. London, U.K.: Research Studies Press, 2003.

[2] E. Macdonald et al., "3D Printing for the Rapid Prototyping of Structural Electronics," in IEEE Access, vol. 2, pp. 234-242, Dec. 2014, doi: 10.1109/ACCESS.2014.2311810.

[3] Keyrouz, S. and Caratelli, D., 2016. Dielectric Resonator Antennas: Basic Concepts, Design Guidelines, and Recent Developments at Millimeter-Wave Frequencies. International Journal of Antennas and Propagation, 2016, pp.1-20.

[4] M. Cuevas, F. Pizarro, A. Leiva, G. Hermosilla and D. Yunge, "Parametric Study of a Fully 3D-Printed Dielectric Resonator Antenna Loaded With a Metallic Cap," in IEEE Access, vol. 9, pp. 73771-73779, 2021, doi: 10.1109/ACCESS.2021.3081068.

[5] Z. -X. Xia, K. W. Leung and K. Lu, "3-D-Printed Wideband Multi-Ring Dielectric Resonator Antenna," in IEEE Antennas and Wireless Propagation Letters, vol. 18, no. 10, pp. 2110-2114, Oct. 2019, doi: 10.1109/LAWP.2019.2938009.

[6] D. Mitra et al., "Conductive Electrifi and Nonconductive NinjaFlex Filaments based Flexible Microstrip Antenna for Changing Conformal Surface Applications," Electronics, vol. 10, no. 7, p. 821, Mar. 2021, doi: 10.3390/electronics10070821.

[7] "FCC C-band regulations" https://www.fcc.gov/document/fcc-opens-100-megahertz-mid-band-spectrum-5g-0 (accesssed Sep. 16, 2022)

[8] M. Yang, Y. Pan and W. Yang, "A Singly Fed Wideband Circularly Polarized Dielectric Resonator Antenna," in IEEE Antennas and Wireless Propagation Letters, vol. 17, no. 8, pp. 1515-1518, Aug. 2018, doi: 10.1109/LAWP.2018.2851574.

[9] "Electrifi website" https://www.multi3dllc.com/product/electrifi/ (accesssed Aug. 20, 2022)

[10] "Premix website" https://www.preperm.com (accesssed Sep. 10, 2022)

[11] A. Goulas et al., "The Impact of 3D Printing Process Parameters on the Dielectric Properties of High Permittivity Composites," Designs, vol. 3, no. 4, p. 50, Nov. 2019, doi: 10.3390/designs3040050.